Mesoporous Microspheres Composed of PtRu Alloy

Junhua Jiang and Anthony Kucernak*

Department of Chemistry, South Kensington Campus, Imperial College London, London SW7 2AZ, United Kingdom

Received November 28, 2003

Mesoporous microspheres of PtRu alloy have been successfully prepared by the electrochemical co-reduction of dihydrogen hexachloroplatinate(IV) and ruthenium trichloride both dissolved in the aqueous domains of the liquid crystalline phase of an oligoethylene oxide surfactant. Scanning electron micrographs reveal that the microspheres have a narrow size distribution in the range 0.5−1 μm. The ordered mesoporous internal structure of the microspheres has been confirmed by transmission electron micrographs and is characterized by periodic pores of ca. 2.4 nm in diameter separated by walls of ca. 2.4 nm thick. X-ray diffraction studies show that a higher Ru content is alloyed in the material than typically found in chemically prepared PtRu catalysts. The specific electrochemical surface area measured using both the CO adsorption and underpotential deposited Cu stripping techniques is 78−81 m^2g^{-1}—much larger than that of unsupported precious metal catalysts produced using standard techniques. The combination of high surface area and periodic nanostructure of this alloy material makes it an interesting prospective fuel cell electrocatalyst. This has been demonstrated by the high activity of the electrodeposited mesoporous PtRu material toward methanol electrooxidation.

Introduction

The synthesis and characterization of mesoporous materials have recently received increased interest because of their potential applications to a wide variety of technologies, such as catalysis, chemical separation, microelectronics, and optics. Mesoporous silica and transition metal oxides have been synthesized by using molecular self-assemblies of surfactants or related substances as templates. This approach has been significantly widened by the introduction of liquid crystal templating materials. Attard and co-workers have used the direct templating method to prepare mesoporous silica[1] and a class of metallic systems.[2−4] Because of the combination of high surface area and periodic nanostructure, mesoporous metallic materials have been studied for applications in fuel cells,[5−9] sensors,[10] batteries, and electrochemical supercapacitors.[11]

Mesoporous metallic systems can be obtained by either chemical or electrochemical reduction of metal compounds dissolved in the aqueous domains of the lyotropic liquid crystalline phases of nonionic surfactants. Electrochemical deposition is ideal for the production of metallic films or powders. Mesoporous single component metallic systems including Pt[2], Sn[4], and Ni[11] have been electrochemically synthesized using the liquid template method. But there has been no report of the electrochemical preparation of nanostructured multicomponent alloys. PtRu alloys are currently the most efficient anode electrocatalysts in low-temperature polymer membrane fuel cells using methanol or reformate as a fuel. The surface morphology, composition, crystalline structure, and nanostructure of the PtRu alloys are of major interest in developing "poison tolerant" fuel cell electrocatalysts.[12−14] Here we report the electrochemical production of mesoporous PtRu alloy microspheres under diffusion control from the lyotropic liquid crystalline phases of octaethylene glycol monoalkyl ethers and their electrocatalytic activity toward methanol electrooxidation. Because of negligible convection, low diffusion coefficients, and high viscosity in the liquid crystalline phase, metal and alloy powders can be easily produced under conditions of predominantly mass transport control at room temperature.

Experimental Section

Chemicals. The surfactant, octaethylene glycol monohexadecyl ether ($C_{16}EO_8$) (98%, Fluka), dihydrogen hexachloro-

* To whom correspondence should be addressed. E-mail: a.kucernak@imperial.ac.uk. Phone: +44 20 7594 5831. Fax: +44 20 7594 5804.

(1) Attard, G. S.; Glyde, J. C.; Goltner, C. G. *Nature* **1995**, *378*, 366.
(2) Attard, G. S.; Bartlett, P. N.; Coleman, N. R. B.; Elliott, J. M.; Owen, J. R.; Wang, J. H. *Science* **1997**, *278*, 838.
(3) Attard, G. S.; Goltner, C. G.; Corker, J. M.; Henke, S.; Templer, R. H. *Angew. Chem., Int. Ed. Engl.* **1997**, *36*, 1315.
(4) Whitehead, A. H.; Elliott, J. M.; Owen, J. R.; Attard, G. S. *Chem. Commun.* **1999**, 331.
(5) Jiang, J.; Kucernak, A. *Electrochem. Solid-State Lett.* **2000**, *3*, 559.
(6) Jiang, J.; Kucernak, A. *J. Electroanal. Chem.* **2002**, *520*, 64.
(7) Jiang, J. H.; Kucernak, A. *J. Electroanal. Chem.* **2002**, *533*, 153.
(8) Jiang, J. H.; Kucernak, A. *J. Electroanal. Chem.* **2003**, *543*, 187.
(9) Kucernak, A.; Jiang, J. H. *Chem. Eng. J.* **2003**, *93*, 81.
(10) Evans, S. A.; Elliott, J. M.; Andrews, L. M.; Bartlett, P. N.; Doyle, P. J.; Denuault, G. *Anal. Chem.* **2002**, *74*, 1322.
(11) Nelson, P. A.; Elliott, J. M.; Attard, G. S.; Owen, J. R. *Chem. Mater.* **2002**, *14*, 524.
(12) Long, J. W.; Stroud, R. M.; Swider-Lyons, K. E.; Rolison, D. R. *J. Phys. Chem. B* **2000**, *104*, 9772.
(13) Vogel, W.; Britz, P.; Bonnemann, H.; Rothe, J.; Hormes, J. *J. Phys. Chem. B* **1997**, *101*, 11029.
(14) Takasu, Y.; Itaya, H.; Iwazaki, T.; Miyoshi, R.; Ohnuma, T.; Sugimoto, W.; Murakami, Y. *Chem. Commun.* **2001**, 341.

10.1021/cm035237j CCC: $27.50
Published on Web 03/09/2004

platinate(IV) hydrate (DHHCP) (99.9%, Aldrich), ruthenium trichloride (Alfa), methyl alcohol (99.9+%, HPLC grade), hydrated cupric sulfate (BDH, AnalaR), and sulfuric acid (BDH, ARISTAR grade) were used as received without further purification. High-purity carbon monoxide (99.95%, BOC gases) was used in CO-stripping experiments. All solutions were prepared using deionized water (18 MΩ cm resistivity, Millipore MilliQ system) and degassed using high-purity argon.

Electrodeposition of Mesoporous PtRu Alloy. The electroplating mixture was a ternary system consisting of 42 wt % of $C_{16}EO_8$, 29 wt % of metal salts, and 29 wt % of deionized water. DHHCP (1.0 g) and $RuCl_3$ (0.51 g) were dissolved in 1.51 g of deionized water. $C_{16}EO_8$ (2.19 g) was added to the solution, and the mixture was mixed vigorously using a glass rod. Then the mixture was sealed in a vial and subjected to three heating/cooling cycles between 20 and 80 °C with vigorous shaking employing a vortex mixer. All mixtures were allowed to equilibrate at room-temperature overnight before use.

The PtRu alloy samples for physical and electrochemical characterization were electrodeposited at a constant potential onto a gold foil of 1.5 × 1 cm^2 at room temperature in a conventional three-electrode configuration with a gold plate counter electrode and a saturated Ag/AgCl reference electrode. After the electrodeposition, the working electrode was removed from the cell and rinsed repeatedly with copious amounts of acetone and then water to remove surfactants and electrolyte. For electrocatalytic activity measurements the PtRu alloy was electrodeposited onto a gold microelectrode (60 μm diameter) at a constant potential of −0.15 V vs Ag/AgCl for 1200 s.

In the following sections electrodeposited mesoporous PtRu is denoted as *H_I-ePtRu*. For the purpose of comparison, chemically synthesized mesoporous PtRu reported in the references is denoted as *H_I-cPtRu*.

Physical and Electrochemical Characterization. Scanning electron microsope (SEM) images were obtained using a LEO 1525 Gemini field emission scanning electron microscope operating at 20 kV equipped with an Inca energy-dispersive X-ray spectroscope (EDXS) (Oxford Instruments). The transmission electron microscope (TEM) images were taken on a JEOL 2000FX transmission electron microscope operating at a voltage of 200 kV. Wide-angle X-ray diffraction (XRD) spectra were measured with a Philips PW1840 diffractometer using Cu Kα radiation.

Specific electrochemical surface area was assessed using CO and underpotential deposited (*upd*) Cu stripping techniques. CO was adsorbed onto the electrode surface by bubbling high-purity CO through the 0.5 mol dm^{-3} H_2SO_4 electrolyte solution bathing the electrode for 12 h while holding the potential at 30 mV vs RHE. After the adsorption, the dissolved CO was removed from the solution by bubbling high-purity argon for 30 min while still holding the potential at 30 mV. The potential was then scanned in a positive direction from 30 mV at 5 mV s^{-1}. The *upd* Cu[15,16] was adsorbed onto the electrode surface by polarizing it at 0.30 V vs RHE for 3 h in a 0.5 mol dm^{-3} H_2SO_4 containing 0.020 mol dm^{-3} $CuSO_4$. The potential was then scanned positively at 5 mV s^{-1}. In both cases the resulting current was integrated after correcting for the contribution of oxide growth and double layer charging currents.

Assessment of Electrocatalytic Activity. Both voltammetric and chronoamperometric measurements were performed in a thermostated three-chamber electrochemical cell with a Luggin capillary and a platinum flag counter electrode using an Autolab general purpose electrochemical system (Ecochemie, Netherlands). A saturated calomel electrode (SCE) was used as the reference electrode. Potentials reported in electrocatalytic measurements are corrected to the reversible hydrogen electrode (RHE) scale.

Base voltammetric measurements were carried out in 0.5 mol dm^{-3} H_2SO_4 free of methanol at 20 °C. All methanol electrooxidation experiments were carried out in 0.5 mol dm^{-3} H_2SO_4 containing 1.0 mol dm^{-3} methanol at 60 °C. Chronoamperometric profiles were measured by applying a potential step program to the electrode similar to the one described in our previous papers.[7,8] Briefly, a single potential step from the open circuit potential (−0.05 V) to 0.80 V was first applied to the electrode in the methanol-containing solution. After a waiting time of 1 s at 0.85 V, the electrode was polarized at 0.04 V for 1 s to reduce any adsorbed oxides or hydroxides formed on the electrode surface at 0.85 V, followed by recording the current transient at different potentials for 100 s.

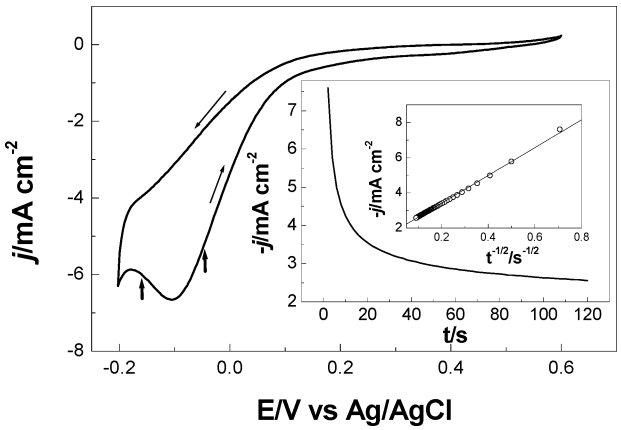

Figure 1. Cyclic volammograms for a gold disk electrode (500 μm in diameter) in a liquid crystalline phase containing 1.32 mol dm^{-3} H_2PtCl_6 and 1.32 mol dm^{-3} $RuCl_3$ at a scan rate of 5 mV s^{-1}. Inset: Current−time transient obtained after stepping the potential from 0.60 to −0.15 V.

Results and Discussion

Figure 1 shows cyclic voltammograms for a gold disk electrode (500 μm diameter) in the electroplating mixture containing DHHCP and $RuCl_3$ at a scan rate of 5 mV s^{-1}. During the negative-going scan reduction commences at about 0.10 V and a reduction peak is seen at about −0.10 V. Such behavior is similar to that seen for a gold electrode in a similar electroplating mixture in the absence of $RuCl_3$.[17] The current−time transient obtained after stepping the potential from 0.60 V to −0.15 V is shown in the inset to this figure. The chronoamperometric current is proportional to the inverse square root of time. This linear relation strongly suggests that the electrodeposition is under diffusion control at potentials more negative of the reduction peak.

The electrodeposition of platinum from the DHHCP precursor may involve the following processes:[18]

$$PtCl_6^{2-} + 2e \rightarrow PtCl_4^{2-} + 2Cl^- \quad E° = 0.726\ V \quad (I)$$

$$PtCl_4^{2-} + 2e \rightarrow Pt + 4Cl^- \quad E° = 0.758\ V \quad (II)$$

$$PtCl_6^{2-} + 4e \rightarrow Pt + 6Cl^- \quad E° = 0.744\ V \quad (III)$$

These electrochemical processes are likely to occur simultaneously during the electrodeposition. A metallic Pt film can be obtained through the electrochemical reduction of DHHCP at about 0.35 V vs RHE.[17] In acidic

(15) Green, C. L.; Kucernak, A. *J. Phys. Chem. B* **2002**, *106*, 1036.
(16) Green, C. L.; Kucernak, A. *J. Phys. Chem. B* **2002**, *106*, 11446.
(17) Elliott, J. M.; Attard, G. S.; Bartlett, P. N.; Coleman, N. R. B.; Merckel, D. A. S.; Owen, J. R. *Chem. Mater.* **1999**, *11*, 3602.
(18) Bard, A. J.; Parsons, R.; Jordan, L. R. *Standard Potentials in Aqueous Solutions*; Marcel Dekker: New York, 1985.

solution $RuCl_3$ may exist in a range of Ru complexes, the most prevalent of which may be abbreviated as $[RuO(H_2O)_4]^{2+}$ in which ruthenium (IV) is present.[19] Metallic Ru is then produced through the following reaction:

$$[RuO(H_2O)_4]^{2+} + 2H^+ + 4e \rightarrow Ru + 5H_2O \quad (IV)$$

The standard potential for the four-electron reduction process may be rather high as the open circuit potential for a Pt electrode in the acidic solution containing the ruthenium complex stabilizes at about 0.83 V.[20] At 0.30 V vs RHE the ruthenium complex can be reduced to metallic Ru.[20] Obviously, at this potential the electrochemical production of PtRu alloy is thermodynamically and kinetically favored. In aqueous solutions the voltammetric reduction waves corresponding to these processes merge together, and PtRu alloys with various compositions and morphologies dependent upon the deposition conditions have been produced.[21,22]

Besides the electrochemical reduction of the ruthenium complex (reaction IV), Ru oxides can be formed through the spontaneous decomposition of the complex and a following electrochemical reaction.[20]

$$[RuO(H_2O)_4]^{2+} \rightarrow RuO_{2,ad} + 3H_2O + 2\,H^+ \quad (V)$$

$$RuO_{2,ad} + 2\,H^+ + 2e \rightarrow RuO_{ad} + H_2O \quad (VI)$$

The percentage of Ru oxides formed in concert with the metallic Ru component is dependent upon the kinetics of reaction IV and reactions V−VI.

Therefore it would be expected that the electrochemical reduction of DHHCP and $RuCl_3$ in the liquid crystalline surfactant phase would produce PtRu alloy and some Ru oxide. The physicochemical properties of the deposit are strongly dependent upon experimental conditions. At low deposition overpotentials the formation of a smooth and compact mesoporous film would be expected, owing to the existence of the templating surfactants which tend to act as leveling agents. Under conditions of high overpotentials the material electrodeposited generally becomes rougher in texture and shows a higher active area. The formation of spherical particles is a mass-transport-controlled phenomenon[23] and is enhanced by having high current densities (i.e., high overpotentials), negligible convection, low diffusion coefficients, and high viscosities—with the latter all being effects that the liquid crystalline phase would favor. Thus, it is unsurprising that mesoporous microspheres are formed under the conditions described in this paper, whereas more compact mesoporous film would be formed under kinetic control at low overpotentials.

In our work the two potentials arrowed in Figure 1 (−0.05 V where the deposition is under mixed diffusion-kinetic control and −0.15 V where the deposition is completely diffusion-controlled) were chosen to produce PtRu deposits. It would be expected that under mass transport limitations preferential formation of a rough film composed of mesoporous spherical particles would occur.

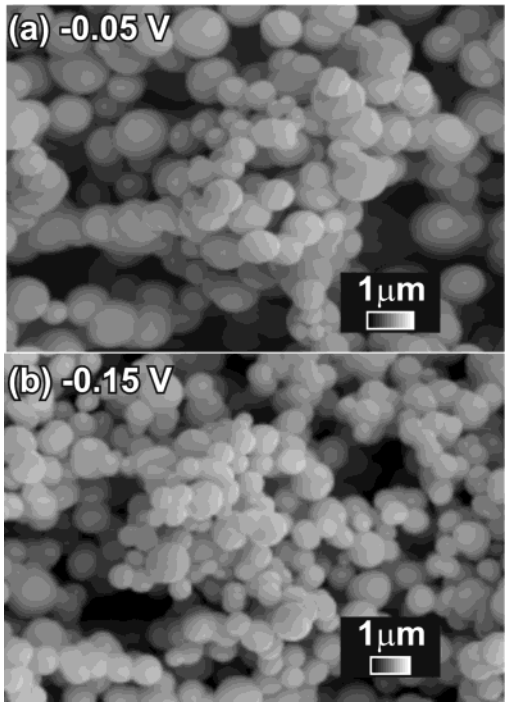

Figure 2. SEM images of *H_I-ePtRu* films deposited at −0.05 (a) and −0.15 V (b).

Scanning electron micrographs clearly show the interesting spherical morphology of the deposits prepared at −0.05 and −0.15 V from the liquid crystalline phases, Figure 2 (a) and (b). The deposits consist of aggregated microspheres with a narrow particle size distribution ranging over 0.5−1.0 μm. It is important to note that these particles are not solid, but have a mesoporous morphology—i.e., each sphere is porous like a sponge. On the outer edge or top of the deposits are a few spherical particles smaller than the particles deposited further into the film. The spherical appearance of the deposits is consistent with the above predictions. Transmission electron micrographs unambiguously reveal a highly porous structure for both deposits as shown in Figure 3 (a) and (b).

The end-on view of a hexagonally closed packed array of pores can be seen in the upper left corner of Figure 3(a). Light color regions correspond to the pores left after removal of the surfactant, whereas dark regions correspond to the deposited alloy. The average diameter of the pores and the thickness of their walls separating them are measured to be 2.4 ± 0.3 nm and 2.4 ± 0.3 nm, respectively. A side view of the hexagonally packed cylindrical pores can be observed in most areas of these TEM images characterized by dark and light parallel lines with a repeat distance of 2.4 ± 0.3 nm. These values are comparable with those found for electrodeposited mesoporous platinum films and chemically synthesized Pt powder from the lyotropic liquid crystalline phases of the same surfactant.[2,3,7,8] On the basis of the pore size and wall thickness, a mesoporous PtRu film with perfect hexagonal nanostructure would be expected to contain 77.4 vol% PtRu and 22.6 vol% pores. The specific surface area inside these pores would be

(19) Gortsema, P. F.; Gobble, J. W. *J. Am. Chem. Soc.* **1961**, *83*, 4317.
(20) Chrzanowski, W.; Wieckowski, A. *Langmuir* **1997**, *13*, 5974.
(21) Quiroz, M. A.; Gonzalez, I.; Meas, Y.; Lamy-Pttara, E.; Barbier, J. *Electrochim. Acta* **1987**, *32*, 289.
(22) Mishima, B.; Mishima, H. T.; Castro, G. *Electrochim. Acta* **1995**, *40*, 2491.
(23) Pletcher, D.; Walsh, F. *Industrial Electrochemistry*, 2nd ed.; Chapman & Hall: London, 1990.

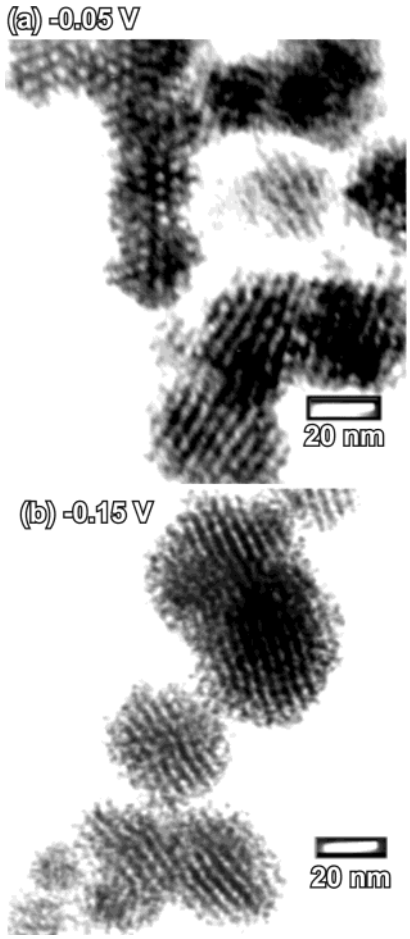

Figure 3. TEM images of H_I-*ePtRu* films deposited at −0.05 (a) and −0.15 V (b).

about 21 $m^2\ g^{-1}$ in a 2-dimensional hexagonal structure. If there are 3-dimensionally interconnected pores, a higher specific pore surface area would be expected.

The compositions of the deposited materials derived from EDXS measurements (not shown) are $Pt_{47.5}Ru_{28.7}O_{23.7}$ and $Pt_{44.5}Ru_{32.8}O_{22.7}$ for the films deposited at −0.05 and −0.15 V, respectively. A high content of oxygen is detected in these deposits, as might be expected if reactions V and VI occurred to a significant extent. The corresponding atomic ratios of Pt/Ru are 62:38 and 58:42.

X-ray diffraction patterns of the mesoporous PtRu deposited at −0.05 and −0.15 V are shown in Figure 4. They display the (111), (200), (220), (311), and (222) reflections characteristic of the face-centered cubic (*fcc*) Pt alloy crystal structure. No indication of a second metallic Ru component is evident. These reflections are in agreement with the characteristic reflections of Pt except that there is some shift in the position of each reflection peak. The higher level of counts seen at low angle is related to the mesoporous structure. The diffraction data are summarized in Table 1. The (111) and (220) peak positions are normally the most reliable for assessment of nanostructured platinum-based catalysts. They give an average lattice parameter of 3.865 and 3.855 Å for the films deposited at −0.05 and −0.15 V, respectively. These values are smaller than the lattice constant of 3.880 Å for chemically synthesized mesoporous $Pt_{50}Ru_{50}$.[24] For unsupported $Pt_{65}Ru_{35}$ catalyst the lattice parameter is measured as being 3.881 Å.[25] This

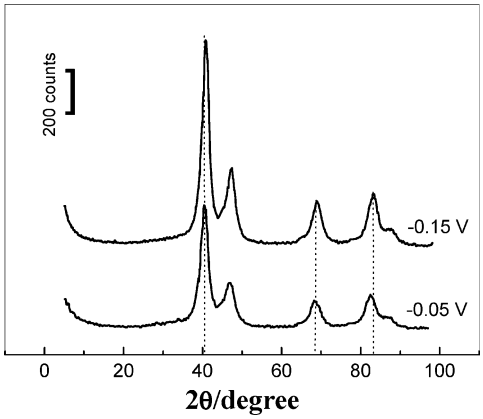

Figure 4. X-ray diffraction patterns of H_I-*ePtRu* films deposited at −0.05 and −0.15 V.

Table 1. Wide-Angle X-ray Diffraction Data for Electrodeposited Mesoporous Pt[22] and PtRu Obtained Using Cu $K_{\alpha 1}$ Radiation

	H_I-*ePt*[22]		H_I-*PtRu* (−0.05 V)		H_I-*PtRu* (−0.15 V)	
hkl	*d*/Å	*I*/au	*d*/Å	*I*/au	*d* (Å)	*I*/au
111	2.25	100	2.23	100	2.23	100
200	1.96	54	1.93	32	1.92	38
220	1.38	29	1.37	14	1.36	25
311	1.19	31	1.16	21	1.16	30

comparison indicates that the nearest-neighbor distance of the H_I-*ePtRu* is reduced by 0.4−0.6% compared to PtRu produced using "normal" methods.

From the values of the lattice parameters, the Ru atomic fraction in PtRu alloy can be assessed. Assuming that the dependence of the PtRu lattice parameter of the mesoporous alloy with Ru content follows the Vegards' law, the lattice constant should follow:[26,27]

$$l_{\mathrm{PtRu}} = l_{\mathrm{Pt}} - k\chi_{\mathrm{Ru}} \qquad (1)$$

where $l_{\mathrm{Pt}} = 3.897$ Å is the lattice parameter of pure mesoporous Pt and $k = 0.124$ Å is a constant. The atomic fractions of Ru in the *fcc* alloy are estimated as being 25.8 and 33.8% for the films deposited at −0.05 and −0.15 V, respectively. They are smaller than the 38 and 42 at. % corresponding to the Ru content of the samples. This implies that the excess Ru must exist as an amorphous oxide. On the basis of the values of χ_{Ru}, the degree of Ru alloyed ($\mathrm{Ru_{al}}$) can be obtained from the following expression:

$$\mathrm{Ru_{al}} = \chi_{\mathrm{Ru}}/[(1 - \chi_{\mathrm{Ru}})(\mathrm{Ru/Pt})_{\mathrm{nom}}] \qquad (2)$$

where $(\mathrm{Ru/Pt})_{\mathrm{nom}}$ is the nominal ratio. The percentage of alloyed Ru is thus 56.9 and 76.9 at. % for the films deposited at −0.05 and −0.15 V, respectively, higher than typically found in the literature data for nanoparticulate PtRu alloys. For example, only 15.9 at. % of Ru is alloyed in chemically synthesized mesoporous $Pt_{50}Ru_{50}$.[24] For carbon supported PtRu, a maximum value of 49 at. % of Ru exists in the PtRu alloy phase after being treated at high temperature.[27] Therefore, the

(24) Attard, G. S.; Leclerc, S. A. A.; Maniguet, S.; Russell, A. E.; Nandhakumar, I.; Bartlett, P. N. *Chem. Mater.* **2001**, *13*, 1444.
(25) Arico, A. S.; Antonucci, P. L.; Modica, E.; Baglio, V.; Kim, H.; Antonucci, V. *Electrochim. Acta* **2002**, *47*, 3723.
(26) Chu, D.; Gilman, S. *J. Electrochem. Soc.* **1996**, *143*, 1685.
(27) Antolini, E.; Cardellini, F. *J. Alloys Compd.* **2001**, *315*, 118.

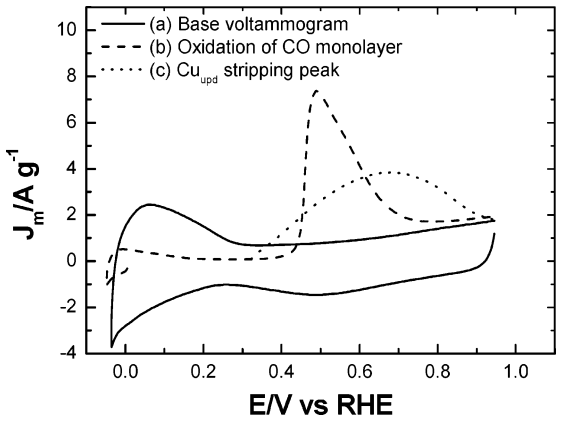

Figure 5. Base cyclic voltammograms (solid line), CO (dashed line), and *upd* Cu (dotted line) stripping voltammograms for an H_I-*ePtRu* film deposited at −0.15 V (dE/dt: 5 mV s^{-1}).

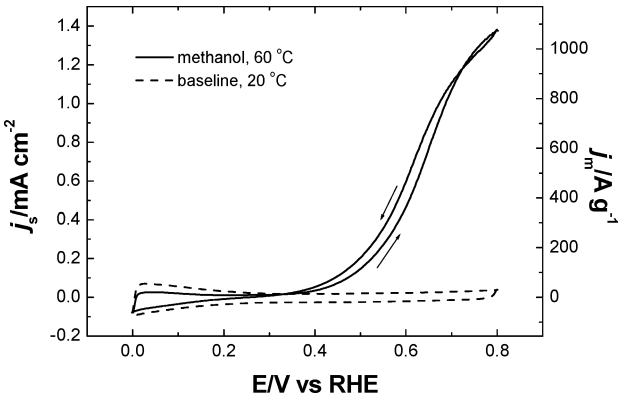

Figure 6. Cyclic voltammograms for H_I-*ePtRu* (0.23 mg cm^{-2}, 170 nm thick) deposited onto a 60-μm-diameter Au microelectrode in 0.5 mol dm^{-3} H_2SO_4 containing 1.0 mol dm^{-3} methanol at 60 °C (dE/dt: 200 mV s^{-1}). Dashed line: base voltammogram.

electrodeposition process described in this paper allows a higher content of Ru to enter the Pt lattice while maintaining the *fcc* crystal structure in the H_I-*ePtRu*. The un-alloyed Ru most likely exists as an amorphous oxide phase which remains undetected in the X-ray diffraction experiment. The atomic ratio of unalloyed Ru to oxygen is about 1:2 indicating that RuO_2 is the predominant oxide. Although RuO_2 could be further reduced to RuO through reaction VI, exposure of this reduced oxide to air after the electrodeposition may lead to reoxidation to form the former material.

The equivalent "particle size" (more correctly, the coherence length of crystalline domains) for both the H_I-*ePtRu* samples is calculated to be about 4.2 nm from measured half-peak width and peak position according to the Debye−Scherrer equation. This figure is close to the sum of pore diameter plus wall thickness—i.e., the notional "repeat distance" of the material.

The hydrogen and oxygen electrochemistry of the H_I-*ePtRu* samples deposited at −0.15 V in 0.5 mol dm^{-3} H_2SO_4 are consistent with literature results obtained under the same conditions,[8,28] as shown in Figure 5. The specific pseudo-capacitance of the film is around 180 F g^{-1} estimated at 0.30 V. The peak potential for oxidation of the CO monolayer is about 0.49 V, close to literature data.[8] On the basis of a theoretical charge of 420 μC cm^{-2} for the stripping of a CO monolayer or a *upd* Cu monolayer, the specific electrochemical surface area of the H_I-*ePtRu* measured from the CO and the *upd* Cu stripping charge is 81.0 and 78.2 m^2 g^{-1}, respectively. These measurements provide a good approximation to the true specific surface area because these techniques give surface areas very close to that calculated using the BET surface area method.[29,30] For chemically synthesized mesoporous PtRu alloy a BET surface area value of 86 m^2 g^{-1} has been reported.[24] These surface area results confirm that the surface area of the H_I-*ePtRu* is highly developed. The specific surface area calculated for the H_I-*ePtRu* is far larger than the value of 21 m^2 g^{-1} estimated for a 2-dimensional hexagonal mesoporous structure, suggesting that there are 3-dimensionally connected pores inside the deposited microspheres.

Figure 6 shows cyclic voltammograms for the mesoporous PtRu film deposited on a gold microelectrode (60 μm diameter) in 0.5 mol dm^{-3} H_2SO_4 containing 1 mol dm^{-3} methanol at 60 °C. Currents are displayed in terms of specific current densities (j_s, current per real surface area) and mass activities (j_m, current per mass of catalyst). The loading of the alloy catalyst is about 0.23 mg cm^{-2} and the film thickness is about 170 nm based on a density of PtRu of 17.83 g cm^{-3} and a volume porosity of 0.23. The electrochemical oxidation of methanol commences at about 0.30 V. This onset potential is a little lower than typical literature data under the same conditions. For chemically synthesized mesoporous PtRu electrocatalyst, the value is about 0.26 V.[8] For unsupported PtRu nanoparticles the onset potential is 0.265 V.[31] During the positive-going scan over the potential range 0−0.80 V, there is no oxidative peak as is usually seen during methanol oxidation at PtRu catalysts. This behavior is different from literature results for supported and unsupported PtRu electrocatalysts, which are characterized by an obvious peak at about 0.76 V and usually ascribed to the blocking of the surface by the formation of oxygen-containing species.[8,32]

Current−time curves as a function of oxidation potential are shown in Figure 7. All the transients are characterized by a rapid current decay at short time followed by the formation of a steady-state current at long time. The currents decay rapidly to zero at potentials more negative than 0.30 V. A steady-state current is attainable at potentials higher than this value. The achievement of a steady-state current indicates that the electrodeposited mesoporous PtRu electrocatalyst has satisfactory CO tolerance. Increasing the potential increases the electrode activity. Utilizing the steady-state currents measured after 100 s polarization, a linear Tafel region is observed over the potential range 0.4−0.55 V (results not shown). The experimental Tafel slope of 126 mV dec^{-1} obtained for this region is close to the theoretical value of 133 mV dec^{-1} at 60 °C for an irreversible one-electron-transfer electrode reaction. This Tafel slope also agrees with literature data for

(28) Antolini, E.; Giorgi, L.; Cardellini, F.; Passalacqua, E. *J. Solid State Electrochem.* **2001**, *5*, 131.
(29) Clair, C. L.; Kucernak, A. *J. Phys. Chem. B* **2002**, *106*, 11446.
(30) Clair, C. L.; Kucernak, A. *J. Phys. Chem. B* **2002**, *106*, 1036.
(31) Park, K.; Choi, J.; Kwon, B.; Lee, S.; Sung, Y.; Ha, H.; Hong, S.; Kim, H.; Wieckowski, A. *J. Phys. Chem. B* **2002**, *106*, 1869.
(32) Tripkovic, A. V.; Popovic, K. D.; Grgur, B. N.; Blizanac, B.; Ross, P.; Markovic, N. *Electrochim. Acta* **2002**, *47*, 3707.

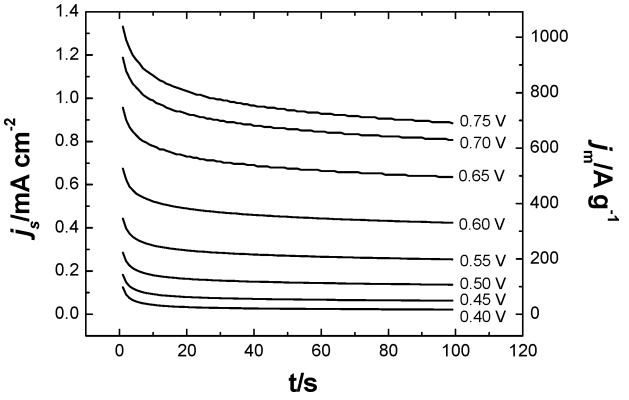

Figure 7. Potentiostatic current−time profiles measured for *H*$_I$*-ePtRu* (0.23 mg cm^{-2}, 170 nm thick) deposited onto a 60-μm-diameter Au microelectrode in 0.5 mol dm^{-3} H_2SO_4 containing 1.0 mol dm^{-3} methanol at 60 °C.

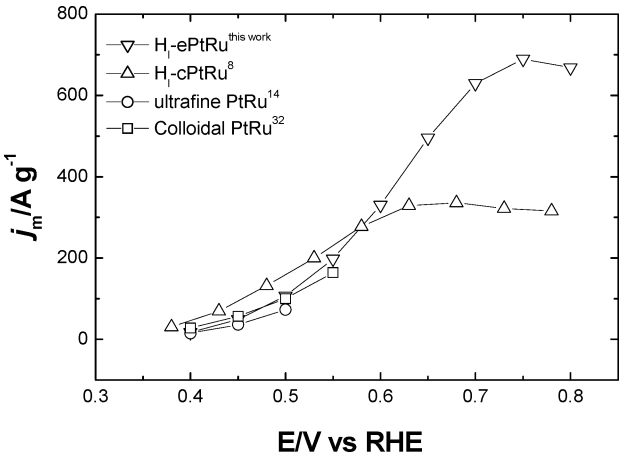

Figure 8. Potential dependence of specific mass activity measured for *H*$_I$*-ePtRu* (0.23 mg cm^{-2}, 170 nm thick) deposited onto a 60-μm-diameter Au microelectrode in 0.5 mol dm^{-3} H_2SO_4 containing 1.0 mol dm^{-3} methanol at 60 °C after 100 s polarization.

methanol oxidation on Pt-based electrocatalysts in acidic media.[8,33] It has been suggested that under these conditions the rate-determining step is the first C−H bond scission linked to a concerted electron charge-transfer process. At more positive potentials the Tafel slope increases to around 223 mV dec^{-1} possibly due to blocking of the electrode surface by the formation of oxygen-containing species or adsorbed anions.

For the purpose of comparison the specific mass activity of electrodeposited mesoporous PtRu and literature data for nanoparticulate PtRu electrocatalysts under the same condition are presented in Figure 8. In the potential range of 0.4−0.55 V, the activity of the *H*$_I$*-ePtRu* electrocatalyst is comparable to that of unsupported PtRu electrocatalysts with a particle size of 2−3 nm.[14,34] But the values are smaller than those of the *H*$_I$*-cPtRu*. At potentials higher than 0.58 V, the electrodeposited *H*$_I$*-ePtRu* electrocatalyst is more active than the *H*$_I$*-cPtRu*. Therefore, the electrodeposited *H*$_I$*-ePtRu* alloy is a potential electrocatalyst toward the methanol electrooxidation reaction especially at high potentials.

Conclusions

Electrochemical deposition of PtRu from metal salts dissolved in the lyotropic liquid crystalline phase of nonionic surfactants provides a productive route to produce mesoporous microspherical catalyst particles with a uniform nanostructured morphology, narrow particle size distribution, and high specific surface area. Under kinetic control smooth and compact films are formed owing to the adsorption of the surfactants on the electrodeposited surface. At higher deposition overpotentials, the electrode reaction becomes diffusion controlled owing to the low diffusion coefficients of the dissolved metal salts and the high viscosity of the deposition solutions. Under such conditions mesoporous microspherical particles are produced. It is possible that such particles can be produced in large scale quantities from the liquid crystalline phase.

Mutiple-component mesoporous microspherical systems would be an interesting class of novel fuel cell electrocatalysts. The electrodeposited PtRu alloy microspherical particles demonstrate high electrocatalytic activity toward the electrooxidation of methanol. Further optimization of the deposition conditions should provide electrocatalysts with higher surface areas, optimized composition, crystalline structure, and morphology.

Acknowledgment. We thank Dr. M. Ardakani and Mr. R. Sweeney for assistance with TEM and X-ray diffraction studies, respectively. The U.K. EPSRC funded this work under grant GR/R19724/01.

CM035237J

(33) Bagotzky, V. S.; Vassiliev, Y. B.; Kazova, O. A. *J. Electroanal. Chem.* **1977**, *81*, 229.

(34) Schmidt, T. J.; Gasteiger, H. A.; Behm, R. J. *Electrochem. Commun.* **1999**, *1*, 1.